Smart Geotechnics for Smart Societies – Zhussupbekov, Sarsembayeva & Kaliakin (Eds)

Innovative geotechnical solution for base isolation

J.S. Dhanya
L. N. Gumilyov Eurasian National University, Astana, Kazakhstan

ABSTRACT: Base isolation systems have been widely recognized as a promising solution for mitigating seismic hazards in buildings. This paper explores a novel solution to the problem of earthquake damage to low-rise buildings in developing countries, where traditional base isolation systems are often too costly and difficult to install. The proposed solution is a Geotechnical Seismic Isolation (GSI) system composed of geomaterials beneath the building foundation to act as a seismic filter medium, reducing the intensity of seismic waves by energy dissipation and damping. The present study focuses on using the Sand-rubber mixture (SRM) and geogrid composite as the geomaterials for energy dissipation. The study includes laboratory tests to optimize the geomaterial composition, scaled model tests, and finite element-based numerical studies to assess the performance of the GSI system under static and dynamic loading. It was observed from the element test that SRM with 30% rubber content has adequate shear strength and damping properties to be used as a foundation bed. The results from scaled model tests on a model footing placed on the GSI system show that a geogrid-reinforced GSI layer can increase bearing capacity up to three times with a significant reduction in settlement. Based on finite element studies on a symmetric low-rise framed building placed on the proposed GSI system subjected to seismic excitation, it was found that GSI is effective in reducing peak ground acceleration and decreasing the shear force and interstory drift in the building.

1 INTRODUCTION

Earthquake-resistant buildings have been a focus for the past few decades. Structural control concepts have been implemented by increasing the strength and stiffness of the structure, but damages can still occur. Though the strengthening method leads to safeguarding the structure from collapse at, the functionality of the structure after an earthquake cannot be guaranteed due to excessive damages. A different approach is to decouple the structure from the footing using base isolation techniques to reduce the intensity of the earthquake vibrations transmitted to the structure. The base isolation systems shift the natural period of the structure, reduce the magnitude of energy transferred to it, and increase damping, reducing the spectral displacement. The first rubber bearing isolator was used in 1969, and by the 1980s, seismic isolation gained worldwide popularity and has been refined over the years, using different types of bearings and materials (Kelly 2002).

Rubber bearings were the first modern-era isolation devices, followed by elastomeric bearings made of rubber and steel layers, which exhibit low damping resistance followed by friction pendulum and sliding bearings. However, the procurement and installation can be costly, making it challenging for developing nations to implement the system for regular residential buildings. A potential alternative to conventional base isolation systems involves incorporating damping into the soil up to a specific depth to partially dissipate energy within the soil before it reaches the foundation and superstructure. Compacted sand layers have traditionally been used as an energy dissipating layer. However, due to the decreasing availability of sand in the construction industry, researchers have investigated the use of waste materials such as scrap rubber tires and other polymeric waste products for geotechnical applications (Edil and

DOI: 10.1201/9781003299127-19

Bosscher1994; Ahn and Cheng 2014). Scrap tires with rubber as their primary component have been found to be particularly useful for vibration isolation (Dhanya et al. 2022, 2020, 2019; Forcellini et al.2020). A mixture of sand and shredded rubber tires, referred to as sand-rubber mixture (SRM), has been proposed as a potential solution to the problems of earthquake hazard, unaffordable and ineffective seismic isolation systems, and the rapid generation of scrap rubber tires. This mixture can be used as a vibration mitigation solution and serves as a novel seismic isolation layer, referred to as the Geotechnical Seismic Isolation (GSI) system, placed below building foundations.

In 2007, Tsang proposed using a sand-rubber mixture (SRM) as a geotechnical seismic isolation layer beneath building foundations. Studies by Tsang et al. (2012,2021), Xiong and Li (2013), and Pitilakis et al. (2015) have demonstrated that this method can reduce both horizontal and vertical shaking levels. Similar studies have examined the use of sandbags and synthetic liners as energy-absorbing layers for seismic protection, with Yegian et al. (2004), Jain et al. (2004), and Ansari et al. (2011) reporting lower accelerations compared to fixed-base structures. Pitilakis et al. (2015) noted that SRM layers are particularly effective for mid-rise buildings, reducing design shear force and displacement. Shaking-table experiments conducted by Xiong and Li (2013) and Bandyopadhyay et al. (2015) with shredded rubber-soil mixtures as isolation material placed below concrete blocks confirm the suitability of SRM for seismic isolation. Previous studies have also reported that the damping ratio of SRM increases with an increment in rubber content (Hazarika et al. 2010; Anastasiadis et al. 2012; Senetakis et al. 2012; Ehsani et al. 2015) and that it has low liquefaction potential (Hazarika et al. 2007; Kaneko et al. 2013; Mashiri et al. 2016). The high elasticity, durability, and non-biodegradability of rubber present in SRM make it a sustainable and cost-effective alternative to expensive base isolation techniques.

The previous studies on the use of SRM for seismic isolation have mainly focused on laboratory characterization of the material with varying amounts and sizes of rubber. However, there is still no conclusive study on the optimal percentage of sand-rubber shreds mixture that provides a reasonable shear modulus with a satisfactory damping ratio over a wide range of strains suitable for seismic isolation applications. Furthermore, limited studies have been reported on the use of SRM as a vibration-absorbing layer for buildings, with little emphasis on site-specific conditions and earthquakes with varying peak ground acceleration (PGA) and frequency content. Additionally, the static performance of buildings placed on the GSI system, settlement problems posed by the low stiffness of SRM, and the influence of Soil-Structure Interaction (SSI) on the performance of the base-isolated building have not been adequately addressed in previous studies.

In view of this, the current study aims to investigate the physical and mechanical response of SRM through a series of laboratory tests to determine the optimal percentage of the mixture that offers sufficient stiffness and energy dissipation capacity. Furthermore, scaled model tests were conducted to evaluate the performance of footings resting on GSI systems, with a primary focus on settlement issues in the foundation on the SRM layer. Geosynthetic reinforcement was also explored to enhance the bearing capacity and settlement performance of the GSI system. Further rigorous dynamic analysis was conducted using advanced Finite Element Method (FEM) tools to gain a deeper understanding of the response of a low-rise building resting on the proposed GSI system under seismic loading.

2 CHARACTERIZATION OF SRM AND GEOSYNTHETIC

The study utilized locally sourced river sand of uniformly angular-shaped grains from Chennai city, India. Scrap rubber tyre used in the study was obtained from a local scrap tyre-recycling unit where the steel reinforcements inside the automobile tyres were removed. The tyre base material used for the study is from heavy-duty automobiles such as lorry/trucks which have a higher proportion of natural rubber compared to other non-rubber ingredients like steel and fibres. The final shredded tyre samples are metal and textile fibre-free. The scrap tyres were fragmented into angular shaped granulated tyres of size less than 4.75 mm using the shredding

machine from the tyre-recycling unit. The tyre particles passing 4.75mm size sieve was used in the preparation of sand-rubber tyre mixture samples. For the present study, the sand and granulated rubber were uniformly hand mixed to achieve a homogenous SRM mixture as shown in Figure 1a. Gravimetric proportioning is adopted rather than the volumetric proportioning for the rubber/sand content in the SRM to attain better control and uniformity in the mixture. The physical properties of sand and the granulated rubber tyre are presented in Table 3.1. The geosynthetic reinforcement used in the study is a commercially available planar biaxial geogrid (MACGRID AR) made of glass fibre strands arranged in grid shape having an aperture size of 10 mm x 10 mm (Figure 1b) with a maximum tensile strength of 11.5 kN/m.

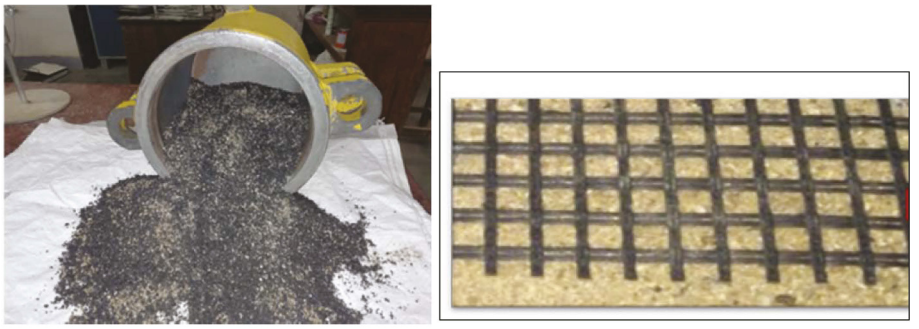

(a) (b)

Figure 1. (a) Typical sand-rubber mixture sample (b) Geogrid used for the study.

To determine the gradation of the material, mechanical shakers were used for grain size analysis (Figure 2a). Based on the Indian standard classification system (IS: 1498 1970), the material was classified as poorly graded Sand (SP). The rubber tyre material used in this study is classified as granulated rubber tyre according to ASTM D 6270-08 (2012) since the particle size lies in the range of 425 μm – 12 mm. The granulated tyre for the present study was classified as an equivalent of poorly graded sand (SP) as per IS: 1498 (1970).

To get a better insight into the effect of rubber content on the shear strength response of the mixture, direct shear test is carried out on a standard apparatus with a shear box of 60 mm x 60 mm size. The shear strength of the mixture was normalized with respect to sand for a relative density of 85%. It can be seen from Figure 2b that the decrease in peak shear strength is gradual upto 30% rubber content, beyond which there is a steep decrease in the strength characteristics. Further, increase in normal stress was found to increase the shear strength of the mixture, this could be due to the redistribution of rubber within the voids of sand particles thereby increasing the contact surface and interlocking friction between sand and rubber particles (Foose et al., 1996; Asadi et al., 2018). Hence for the GSI system in the present study SRM with 30% rubber contend was adopted.

3 SCALED MODEL TEST ON FOOTING RESTING ON GSI SYSTEM

To shed insight into the understanding of shallow foundation performance with the presence of reinforced and unreinforced GSI layer, a series of laboratory model tests were carried out on scaled-down model footing. The study employed Wood's (2004) scaling laws of similitude to ensure similarity in both geometry and materials. A scale factor (λ) of 10 was applied to create a model footing that represents a prototype footing of 1 m x 1 m in size. The prototype footing used concrete with E of 20 GPa, while the model footing used steel with E of 200 GPa. The thickness of the model footing was calculated as 10 mm for the study.

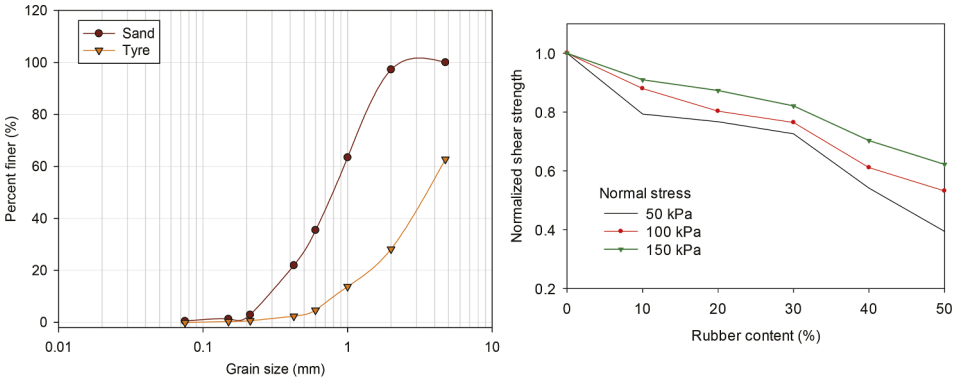

Figure 2. (a) Grain size distribution curve (b) Influence of rubber content on the shear strength of SRM (relative density- 85%).

3.1 *Experimental setup and methodology*

Experiments were conducted using a model square footing of width 0. 1 m (B) placed on top of the GSI layer composed of SRM within a sand bed tank setup (refer to Figure 3). The test tank utilized in this study was made of steel and had inner dimensions of 1 m x 1 m x1 m positioned below a 2m long and 2m high reaction frame. Pneumatic actuators were attached to the reaction frame to apply loads. A steel rod with a height of 1m connected the steel plate for the model footing to the actuator. The pneumatic actuator was used to apply vertical loading in displacement control mode. The load was measured using an electronic load cell with a capacity of 20 kN, and displacement was measured using a linear variable displacement transducer (LVDT) with a capacity of ±30 mm. Calibration of the load cell and LVDT was performed during installation by the equipment providers, and digitalized load-displacement data was automatically saved and available for analysis after testing.

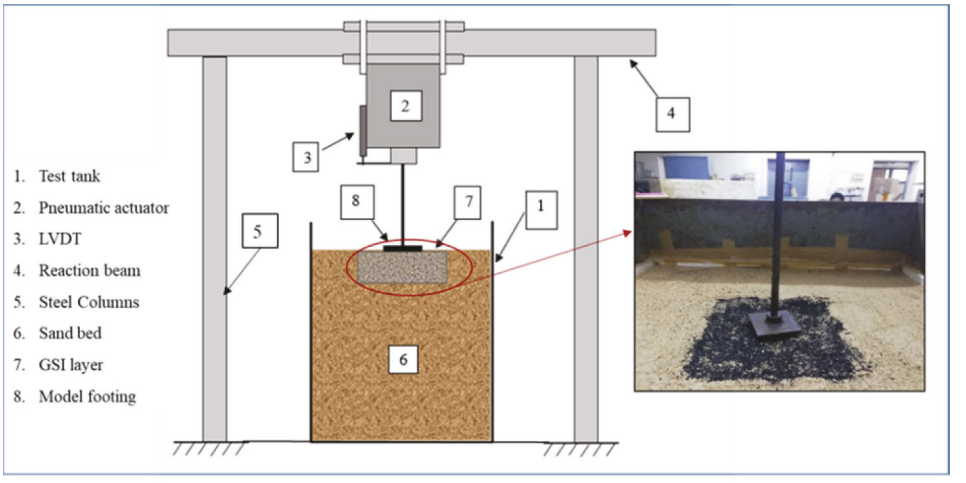

Figure 3. Schematic of the model test setup.

In all experiments, the test tank was filled with sand to a depth of 0.9 meters. A series of tests were conducted on footings resting on different layers of the GSI system to study their behavior under static loading. The first series of tests involved footings on sand beds of 0.9m depth with a relative density of 85% using the sand pluviation technique (Cresswell et al. 1999), where the

sand was poured from a fixed height. The sand was filled in 0.1 m layers and leveled before adding the next layer. Three preliminary trial tests were carried out to confirm the repeatability of load testing. The second series of tests were carried out on footings placed on the SRM-GSI layer. The already-compacted sand bed was excavated for a fixed size of 300 mm x 300 mm with the necessary thickness and backfilled with SRM. Geogrid reinforcement was added to the GSI layers below the footing to increase the bearing capacity and settlement aspect of the system. Hence, the third series of tests were carried out on footings placed on geogrid-reinforced SRM-GSI layer layers. Geogrids were placed at the top of the already compacted sand and SRM layer at a desired depth, and filling was carried out simultaneously to achieve the required relative density. The delicate strain gauges attached to the geogrids were carefully protected throughout the operation to avoid damage. The effective depth of influence is within a range of 2B from the bottom of the footing; hence the geogrids were positioned within a depth of 2B below the footing. In this study, single and double geogrids were used to reinforce the GSI system with layer thicknesses of 1B, 2B and 3B. The single layer of geogrid was placed at a depth of 0.5B, while the double layered geogrids were placed at depths of 0.3B and 0.5B with a vertical spacing of 0.2B. The model footing was placed on the level surface at the center of the GSI layer and sand-bed medium, to which a vertical compressive load was applied until the ultimate bearing pressure was observed. Readings from the load cell, LVDT and strain gauges were collected at a sampling rate of 5s.

3.2 *Response of footing resting on the reinforced and unreinforced GSI layer*

The results obtained from different series of tests are plotted as bearing pressure against the footing settlement (s) in terms of settlement ratios (s/B), as shown in Figure 4. The results revealed that the SRM-GSI layer had a larger settlement compared to the sand layer. The settlement ratio corresponding to the ultimate bearing pressure was 9% for sand and 13% for the SRM-GSI layer. The SRM-GSI layer showed initial compression due to the higher ductility of the rubber content in the mixture. However, there was no significant reduction in the bearing capacity of the GSI layer compared to sand. Interestingly, the SRM-GSI layer with a thickness of 0.5B exhibited a bearing capacity equivalent to that of pure sand. This could be because of the small difference in shear strength between the sand and SRM mixture at lower confining pressure. The bearing capacity of the SRM-GSI layer with a thickness of 1B and 2B increased, but the rate of increment in bearing capacity with settlement ratio reduced by 30% compared to the SRM-GSI layer with 0.5B width. In conclusion, the results suggest that the SRM-GSI layer has a higher settlement than the sand layer.

Figure 4.b Illustrates the load-settlement curves for a footing on the SRM-GSI layer reinforced with geogrid. The results show that the geogrid reinforcement significantly increases the bearing capacity and reduces the settlement of the footing. Additionally, the geogrid-reinforced GSI system exhibits a higher ultimate capacity and fails at higher values of settlement ratio compared to the unreinforced system. The figure reveals that the ultimate bearing capacity of the footing (at an s/B ratio of 20%) on the GSI system increases three times for double geogrids and two times for single geogrid reinforcement. The details of the influence of different parameters of geogrid reinforcement in the GSI system can be found in Dhanya et al. (2019). The studyconfirms that geogrid reinforced GSI system performs well under static loading conditions and can sustain foundation loading sufficiently with adequate bearing capacity and reduced settlement.

4 SEISMIC RESPONSE OF FRAMED STRUCTURE RESTING ON GEOGRID REINFORCED GSI LAYER

A low-rise building with shallow footing is used to numerically analyze the GSI system's dynamic performance using finite element software ABAQUS 6.14. A typical moment resisting framed structure on raft footing is chosen for numerical modeling, with the GSI layer placed below and at the sides of the raft footing. Geogrid reinforcement is added to enhance the GSI system's advantages under static and dynamic loading conditions. The study focuses on a region-specific layered soil domain in the highly seismic Indo-Gangetic plain basin the details of which are presented in Dhanya et al. (2020).

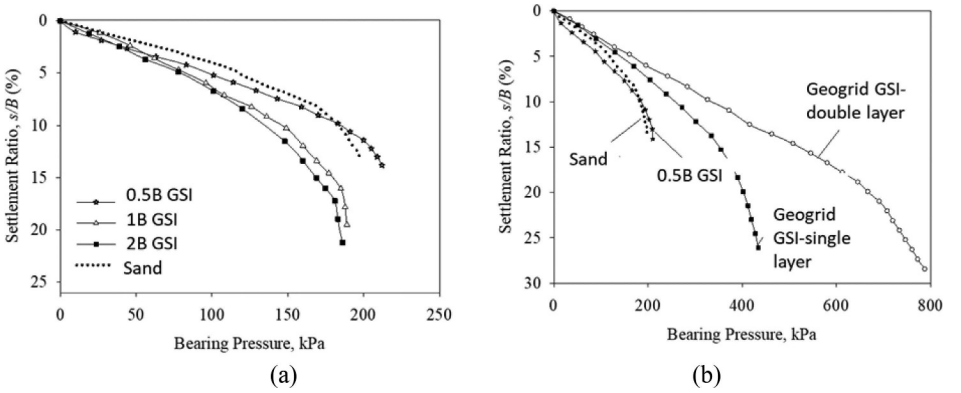

Figure 4. Bearing pressure-settlement response for the GSI system.

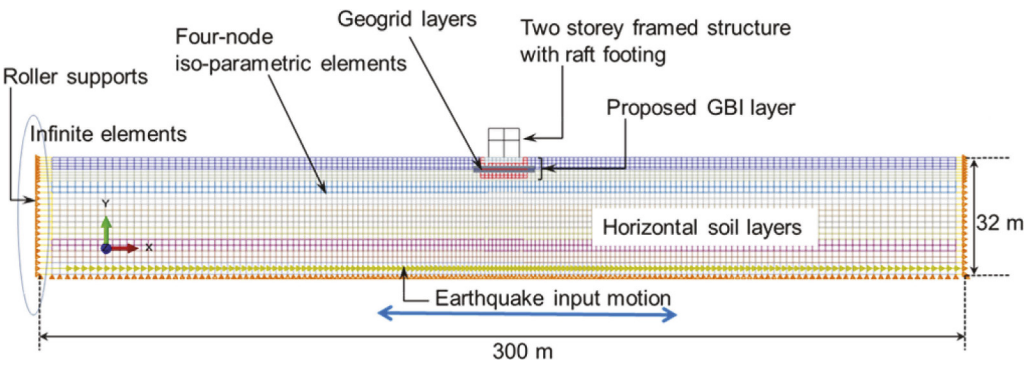

Figure 5. Finite element model adopted for the study.

A-4 type residential apartment buildings with two stories were selected to represent conventional low-rise buildings, based on the National Building Code (NBC) of India (2016). The framed structure used in the study had a height of 4.5 meters at the ground floor (including plinth level) and 3 meters at the top floor, with two equal bays each having a width of 4 m. The beams and columns in the structure were assigned cross-sections of 0.35 m x 0.4 m and 0.35 m x 0.45 m, respectively. The dead load and live load coming on the structure was calculated based on the code provision, IS 875:1987 Part 1& II (2008).

The soil domain of depth 32 m was chosen for the study. Plane strain quadrilateral grids with four-node iso-parametric elements were used to model the soil, GSI layer and footing. Soil is modelled using hypoelstic constitutive model while SRM is modelled using hyperelastic model. Elastic-perfectly plastic material constitutive behaviour was assumed for geogrids modelled using beam elements the details of which can be found in Dhanya et al. (2020). The soil domain was divided into homogenous horizontal layers. The bottom boundary was assumed to be fixed while the side boundaries were given roller supports that restrained horizontal movements but allowed for vertical movements. To simulate unbounded soil media and prevent wave reflections, infinite elements were used to create transmitting boundaries. In the dynamic analysis, the input motions under consideration consist of acceleration-time histories from two major earthquakes that occurred in the Indian subcontinent namely the 2001 Bhuj earthquake (Mw=7.7; PGA=0.1g; predominate frequency= 3.5 Hz) and 2015 Nepal earthquake (Mw=7.8; PGA=0.14g; predominate frequency= 0.2 Hz) obtained from the COSMOS Virtual Data Center as shown in Figure 6.

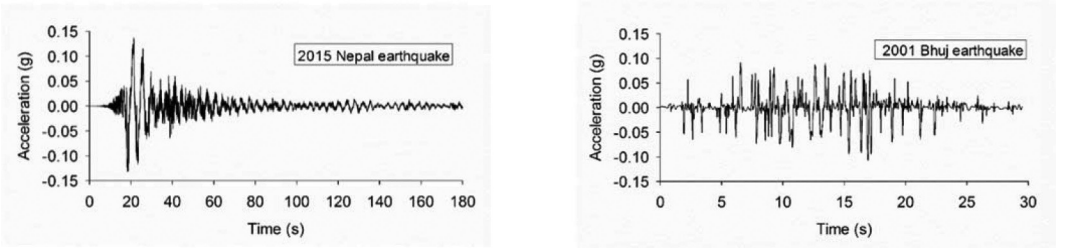

Figure 6. Acceleration-time history of earthquake input motions adopted.

4.1 *Acceleration response of the framed structure on GSI system*

Figure 7a depicts the acceleration-time history obtained at the top of the footing for the natural soil and geogrid reinforced GSI layer of thickness 0.05B when subjected to the 2015 Nepal earthquake motion. The GSI layer shows a significant reduction in the amplitude of acceleration at the footing top compared to the natural soil system. Figure 7b can provide a useful understanding of the characteristics of the acceleration response spectra (with 5% damping) for buildings resting on the geogrid reinforced GSI layer at the footing level. The graph clearly shows a reduction in spectral acceleration for the GSI system compared to the natural sol layer. This reduction is particularly pronounced in the mid-period range of 0.3 s to 1 s, whereas for periods less than 0.3 s and greater than 1 s, the reduction in spectral acceleration is less noticeable. Additionally, the presence of the GSI layer causes a slight shift in the predominant period of the system to a higher value compared to the natural soil system. This shift results in a reduction of spectral acceleration for low-rise buildings, which have a shorter natural period, such as 0.24 s in the current scenario.

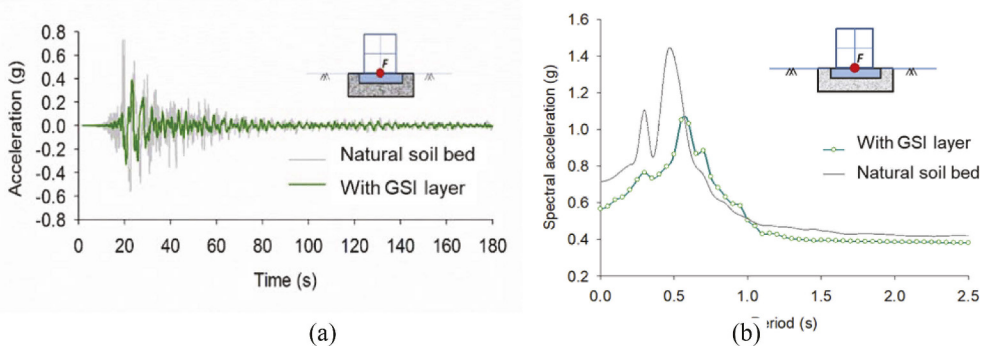

Figure 7. (a) Acceleration time history response (b) Spectral acceleration response at the footing level of the structure.

The thickness of the GSI system has a significant impact on the degree of reduction in earthquake input motion amplification. An optimal thickness of the GSI layer was determined through numerical analysis to ensure satisfactory seismic isolation for the proposed building. The GSI layer thickness was varied at 0.05B, 1B, and 2B, and the system was double-layer geogrid reinforced. The study used the scaled acceleration-time history of the 2015 Nepal earthquake (Mw=7.8) as the input motion and the results were extracted from nodes at the top of the building and footing. The reduction in the peak values of the spectral acceleration due to the presence of GSI was evident for all thicknesses of the GSI layer, as shown in Table 1. The reduction in spectral acceleration values for the GSI system indicates higher energy absorption induced by a thicker layer of the GSI system. For instance, at the top of the building, the isolation efficiency increased by 37% when the thickness of the GSI layer was

increased from 0.05B to 2B. At the footing top, an isolation efficiency of 35% was obtained, indicating that the peak ground acceleration of incoming seismic waves was reduced significantly due to the presence of the GSI layer (thickness=2B). Although the isolation effect initially increases with the increase in thickness of GSI, the isolation efficiency for 0.1B and 0.2B are more or less similar, indicating that using a 0.1B thickness of the GSI layer is enough to achieve the necessary energy dissipation. Additionally, the shift in the fundamental period of the system is more significant for thickness of GSI of 0.1B and 0.2B compared to 0.05B.

Table 1. Effect of thickness of GSI layer on peak spectral acceleration and predominant period (Scaled 2015 Nepal earthquake, Mw=7.8; PGA= 0.24g).

		Peak spectral acceleration (g)		Predominant period (s)	
Description		Footing top	Building top	Footing top	Building top
Natural soil		2.39	2.75	0.47	0.67
Geogrid reinforced GSI layer	$T_{GSI}=0.05B$	1.72	2.27	0.6	0.85
	$T_{GSI}=0.1B$	1.59	1.73	0.67	0.90
	$T_{GSI}=0.2B$	1.46	1.69	0.7	0.95

4.2 *Shear force and interstorey drift*

The effect of seismic isolation on the base shear of the framed structure was investigated and comparison was made between the fixed base structure and structures with seismic isolation, namely, while taking into account the effects of SSI. A constant scaled PGA of 0.24g was maintained for the earthquake input motions during the study. Figure 8 illustrates the base shear ratio, which represents the ratio of shear force developed in the SSI structure to that of the fixed base structure. The figure suggests that the SSI effects are advantageous for the GSI system, as it reduces the base shear when compared to the fixed base system. Additionally, the figure shows that the reduction in base shear is more significant for buildings placed on the SRM-GSI system than on the geogrid reinforced SRM-GSI system. This may be due to the decrease in soil stiffness beneath the building foundation. In contrast, the natural soil layer demonstrated a higher base shear ratio, as it is relatively stiff compared to the GSI system. For example, during the 2015 Nepal earthquake (Mw=7.8), the base shear ratio was 0.47 for the Sur system, which decreased to 0.3 for the GSIur system. Furthermore, the flexible-base provided by the GSI layer influences the SSI effects, resulting in lower base shear when compared to the fixed base system.

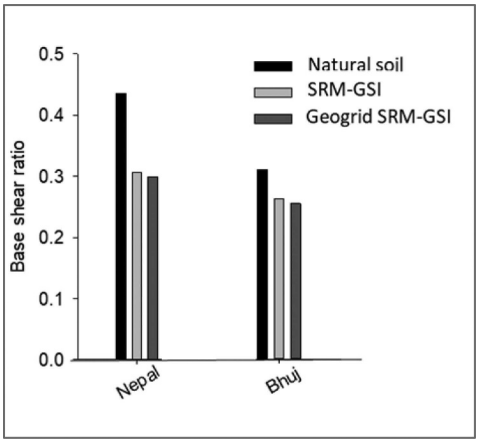

Figure 8. Base shear ratio for different earthquake input motion.

Assessing the performance of GSI isolated structures during earthquakes involves analyzing the maximum lateral displacement experienced by each floor of the building and the corresponding interstorey drift calculated as the difference in lateral deflection of the jth storey and the lateral displacement of the (j+1)th storey, divided by the storey height. The results were summarized in Table 2, which showcases the variation of maximum storey drift for the 1st and 2nd floors of the building for different ground motions (PGA=0.24g). The structure on natural soil had a higher inter-storey drift due to increased lateral displacement in comparison to SRM-GSI layer. This effect is mainly caused by the high amplitude of seismic waves reaching the structure. To further reduce the lateral displacement of GSI layers, the geogrids were introduced, which created a confining effect and restrained the structure's lateral displacement placed on the GSI system.

Table 2. Maximum inter-storey drift of the building for different earthquake motions.

	Maximum storey drift (mm)					
	Natural soil		SRM-GSI		Reinforced SRM-GSI	
Earthquake	1st floor	2nd floor	1st floor	2nd floor	1st floor	2nd floor
2015 Nepal (Mw=7.8)	9.4	10.5	7.7	8.6	6.1	6.6
2001 Bhuj (Mw=7.7)	3.6	5.1	3.2	4.5	3.0	4.2

5 CONCLUSIONS

The present study explores the use of geo-base isolation system made of Sand-Rubber Mixture (SRM) as a vibration isolation layer below the foundation system for seismic protection of buildings using element tests, laboratory model studies and numerical investigation. It was observed that the contribution of sand and rubber to the SRM material matrix is predominant at rubber content below 40% higher than which the influence of rubber matrix prevails. SRM with 30% rubber content possesses adequate stiffness, shear modulus and damping properties ideal for its use as geo-base isolation material. From the model tests, it was observed that the introduction of the proposed GSI layer between the footing and the underlying sandy strata reduces bearing capacity and increases settlement. Provision of geogrids to the geo-base isolation system was found to increase the bearing capacity by two times for single geogrid layer and three times for double geogrid layer. Further, single and double layered geogrid reinforcement reduces the settlement of GSI system up to 30% and 45% respectively. The finite element based numerical studies recommended. It is recommended to adopt the geo-base isolation system for seismic protection of low-rise symmetric buildings in the seismically active Indo Gangetic region of India with the following parameters: GSI layer with a width of 1.2B and thickness of 0.1B reinforced with two layers of geogrid having a spacing of 0.05B and length of 2B.

REFERENCES

Ahn, I. and Cheng, L. (2014). Tire derived aggregate for retaining wall backfill under earthquake loading. *Const. and Building Mat*., 57, 105–116.

Anastasiadis, A., Senetakis, K. and Pitilakis, K. (2012). Small-strain shear modulus and damping ratio of sand-rubber and gravel-rubber mixtures. *Geotech. and Geological Eng*., 30(2), 363–382.

Bandyopadhyay, S., Sengupta, A. and Reddy, G. R. (2015). Performance of sand and shredded rubber tire mixture as a natural base isolator for earthquake protection. *Earthq. Eng and Eng. Vibration*, 14 (4), 683–693.

BIS (Bureau of Indian Standards). 1970. *Classification and identification of soils for general engineering purpose*. IS:1498-1970. Manak Bhawan, New Delhi: BIS.

Cresswell, A., M. E. Barton, and R. Brown. 1999. Determining the maximum density of sands by pluviation. *Geotech. Test. J*. 22 (4): 324–328.

Dhanya, J. S., A. Boominathan, and S. Banerjee. 2019. Performance of geo-base isolation system with geogrid reinforcement. *Int. J. Geo- mech*. 19 (7): 04019073.
Dhanya, J. S., A. Boominathan, and S. Banerjee. 2020. Response of low- rise building with geotechnical seismic isolation system. *Soil Dyn. Earthquake Eng*. 136: 106187.
Dhanya, J. S., A. Boominathan, and S. Banerjee. 2022. Investigation of geotechnical seismic isolation bed in horizontal vibration mitigation. *J. Geotech. Geoenviron. Eng*., 2022, 148(12): 04022108.
Edil, T., and P. J. Bosscher. 1994. Engineering properties of tire chips and soil mixtures. *Geotech. Test. J*. 17 (4): 453–464.
Ehsani, M., Shariatmadari, N. and Mirhosseini, S. M. 2015. Shear modulus and damping ratio of sand-granulated rubber mixtures. *J. Cent. South Univ*., 22, 3159–3167.
Forcellini, D. 2020. Assessment of geotechnical seismic isolation (GSI) as a mitigation technique for seismic hazard events. *Geosciences*, 10 (6): 1–14.
Hazarika H, Yasuhara K, Kikuchi Y, Karmokar AK, Mitarai Y. 2010. Multifaceted potentials of tire-derived three dimensional geosynthetics in geotechnical applications and their evaluation. *Geotext Geomembr*., 28:303–15.
IS 875: 1987 Part 1 (2008). *Code of Practice for Design Loads (Other than Earthquake) For Buildings and Structures. Part 1: Dead Loads-Unit Weights of Building Materials and Stored Materials*. Bureau of Indian Standards, New Delhi.
IS 875: 1987 Part 2 (2008). *Code of Practice for Design Loads (Other than Earthquake) For Buildings and Structures. Part 2: Imposed Loads*. Bureau of Indian Standards, New Delhi.
Jain, S. K. and Thakkar, S. K. (2004). Application of base isolation for flexible buildings. *13th World Conference on Earthquake Engineering*, Vancouver, B.C, Canada, August, Paper no. 1924.
Kaneko, T., Orense, R. P., Hyodo, M. and Yoshimoto, N. (2013). Seismic response characteristics of saturated sand deposits mixed with tire chips. *J. Geotech. Geoenvironmental Eng*., 139(4), 633–643.
Kelly, J. M. (2002). Seismic isolation systems for developing countries. *Earthquake. Spectra*, 18, 385–406.
NBC (2016). *National Building Code of India*. Bureau of Indian Standards (BIS) New Delhi
Pitilakis, K., S. Karapetrou, and K. Tsagdi. 2015. Numerical investigation of the seismic response of RC buildings on soil replaced with rubber– sand mixtures. *Soil Dyn. Earthquake Eng*. 79 (Dec): 237–252.
Rao, G. V., and R. K. Dutta. 2006. Compressibility and strength behaviour of sand-tyre chip mixtures." *Geotech. Geol. Eng*. 24 (3): 711–724.
Senetakis K, Anastasiadis A, Pitilakis K, Souli A. 2012. Dynamic behavior of sand/ rubber mixtures, Part II. *J ASTM Int*., 9(2), 1–13.
Tsang, H. 2008. Seismic isolation by rubber–soil mixtures for developing countries. *Earthquake Eng. Struct. Dyn*. 37 (2): 283–303.
Tsang, H. H., D. P. Tran, W. Y. Hung, K. Pitilakis, and E. F. Gad. 2021. Performance of geotechnical seismic isolation system using rubber-soil mixtures in centrifuge testing. *Earthquake Eng. Struct. Dyn*. 50 (5): 1271–1289.
Tsang, H., Lo, S. H., Xu, X and Sheikh, M. N. (2012). Seismic isolation for low-to-medium-rise buildings using granulated rubber – soil mixtures: numerical study. *Earthquake Eng. Struct. Dyn*., 41, 2009–2024.
Wood, D. M. 2004. *Geotechnical modelling*. Abingdon, UK: Spon.
Xiong, W. and Li, Y. (2013). Seismic isolation using granulated tire–soil mixtures for less-developed regions: experimental validation. *Earthquake Engineering and Structural Dynamics*, 42, 2187–2193
Yegian, M. K. and Kadakal, U. (2004). Foundation isolation for seismic protection using a smooth synthetic liner. *Journal of Geotechnical and Geo-Environmental Engineering*, 130(11), 1121–1130.